Universität Potsdam

Oliver Reich, Hans-Gerd Löhmannsröben, Frank Schael

Optical sensing with photon density waves: investigation of model media

Optical sensing with photon density waves: Investigation of model media†

Oliver Reich, Hans-Gerd Löhmannsröben* and Frank Schael‡

University of Potsdam, Department of Chemistry, Karl-Liebknecht-Str. 24-25, D-14476 Potsdam, Germany. E-mail: loeh@chem.uni-potsdam.de

Investigations with frequency domain photon density waves allow elucidation of absorption and scattering properties of turbid media. The temporal and spatial propagation of intensity modulated light with frequencies up to more than 1 GHz can be described by the P1 approximation to the Boltzmann transport equation. In this study, we establish requirements for the appropriate choice of turbid model media and characterize mixtures of isosulfan blue as absorber and polystyrene beads as scatterer. For these model media, the independent determination of absorption and reduced scattering coefficients over large absorber and scatterer concentration ranges is demonstrated with a frequency domain photon density wave spectrometer employing intensity and phase measurements at various modulation frequencies.

1 Introduction

The employment of optical sensors is often advantageous due to their sensitivity, selectivity and their real time, *in situ* and online capabilities.[1] The optical properties of real world samples are usually of considerable complexity, often causing a combination of absorption, scattering and luminescence. This creates a demand for the independent determination of parameters characterizing these processes. Since the early 1990s, frequency domain (FD) photon density waves (PDW) have been used for the investigation of absorption and scattering properties of turbid media,[2–5] mainly in biomedical sensing.[6,7] Apart from that, other issues addressed with FD-PDW so far include, *e.g.*, investigations of pharmaceutical powders and electrostatic interactions in colloidal systems.[8,9] Conditions for the successful application of PDW are low absorption and strong scattering. This is often found in the red to near infrared spectral region, where absorption and luminescence of many samples is low. Our FD-PDW spectrometer allows investigations in the large frequency range from 0.3 to 1300 MHz with up to 1600 different modulation frequencies. This provides data sets large enough for comprehensive characterization of challenging samples. The theoretical description is based on the so-called P1 approximation to the Boltzmann transport equation. In order to understand the potential of PDW spectroscopy, a delineation of absorption and scattering in well characterized model media is indispensable. In this contribution we discuss requirements for the appropriate choice of compounds for turbid model media, and characterize a mixture of isosulfan blue (ISB) as absorber and polystyrene beads (PS-beads) as scatterer. Different absorber and scatterer concentrations are used to show the applicability of PDW for the determination of the absorption and reduced scattering coefficients of the samples.

2 Theory

In an absorbing and scattering medium, in which the concentration of the scatterers or the optical path length l are so low that only single scattering occurs, the extinction E of a sample measured in transmission is given by:

$$E = (\mu_a + \mu_s)l \tag{1}$$

Here, μ_a and μ_s denote the absorption and scattering coefficients, which equal the inverse lengths after which the incident light intensity is reduced to $1/e$ by the corresponding process. According to the Beer–Lambert law, μ_a and μ_s are, at least for low concentrations, proportional to the molar concentrations of the absorbing species [Abs] or the volume fraction of the scattering species [Sca], respectively:

$$\mu_a = \sum_i \varepsilon_i [\text{Abs}]_i \tag{2}$$

$$\mu_s = \sum_i s_i [\text{Sca}]_i \tag{3}$$

The ε_i are the molar absorption coefficients (*e.g.* in units of $\text{mm}^{-1}\,\text{M}^{-1}$) of the absorbing species and the s_i are the specific scattering coefficients (*e.g.* in units of mm^{-1}) of the scattering species. The single-scattering condition of eqn. 1 is fulfilled for $\mu_s l \ll 1$. Thus, a small optical path length has to be used for the investigation of strongly scattering samples. Nevertheless, minimization of l is often difficult and also lowers the sensitivity of absorption measurements. Alternatively, approaches as PDW spectroscopy are promising, which do not exclude but take advantage of multiple scattering.

Following the treatment of Fishkin *et al.*,[10] the temporal and spatial propagation of light in a multiply scattering medium can be described by the so-called P1 approximation to the Boltzmann transport equation. Assumptions include weak absorption ($\mu_a \ll \mu_s$), large distances to boundaries and light sources, and neglect of polarization and interference effects. For an isotropic point light source one obtains in a three

dimensional representation:[10]

$$-D\nabla^2\rho(\boldsymbol{r},t) + c\mu_{\mathrm{a}}\rho(\boldsymbol{r},t) + \left(\frac{3\mu_{\mathrm{a}}D}{c}+1\right)\frac{\partial}{\partial t}\rho(\boldsymbol{r},t) + \frac{3D}{c^2}\frac{\partial^2}{\partial t^2}\rho(\boldsymbol{r},t)$$
$$= \frac{3D}{c^2}\frac{\partial}{\partial t}s_0(\boldsymbol{r},t) + s_0(\boldsymbol{r},t) \quad (4)$$

$\rho(\boldsymbol{r},t)$ and $s_0(\boldsymbol{r},t)$ are the photon density and the source term as a function of position $\boldsymbol{r}$ (vector) and time t. The speed of light c in a medium is $c = c_0/n$, with the speed of light in vacuum c_0 and the real part of the refractive index of the medium n. D is the optical diffusion coefficient:

$$D = \frac{c}{3(\alpha\mu_{\mathrm{a}} + \mu'_{\mathrm{s}})} \quad (5)$$

$\mu'_{\mathrm{s}} = (1-g)\mu_{\mathrm{s}}$ is the reduced scattering coefficient, and the anisotropy factor g is the intensity-weighted mean cosine of the scattering angle. The anisotropy factor depends, besides the refractive indices of the scatterer and of the medium, mainly on the particle size. Values of g can be obtained from Mie theory[11] and range between -1 (back scattering) and $+1$ (forward scattering). In order to obtain consistency with the units of chemical diffusion coefficients, in our treatment D includes c, which deviates from the expressions given by Fishkin et al.[10] In the literature there is still a dispute about the value of α, which describes the dependance of the diffusion coefficient on the absorption. From former investigations,[12] we concluded that $\alpha = 0.33$ should be preferred instead of the also commonly used values of 0 or 1. This is also supported by the work of Durian.[13]

For an intensity modulated point light source located within the medium, the solution of the integro-differential equation eqn. 4 leads to the following expressions for the time-dependent part of the photon density $\rho_{\mathrm{AC}}(r,t)$ in large distances to sources and boundaries. Due to the spherical symmetry, the expression can be given as a function of the distance r (scalar) to the source instead of $\boldsymbol{r}$.

$$\rho_{\mathrm{AC}}(r,t) = \frac{C}{r}\exp[-k_{\mathrm{I}}r + \mathrm{i}(k_{\Phi}r - \omega t - \Phi_0)] \quad (6)$$

ω is the angular modulation frequency and C depends on the power and modulation depth of the source and the optical parameters of the medium, but neither on r or t. Φ_0 is the phase offset due to the overall electrical and optical path length outside the sample. The most accessible information about scattering and absorption properties is contained in the intensity and phase coefficients k_{I} and k_{Φ}, respectively. They are given by:

$$k_{\mathrm{I}} = \left(\frac{1}{2c^2D}\left([(c^3\mu_{\mathrm{a}} - 3\omega^2D)^2 + (c^2\omega + 3c\omega\mu_{\mathrm{a}}D)^2]^{1/2}\right.\right.$$
$$\left.\left. + (c^3\mu_{\mathrm{a}} - 3\omega^2D)\right)\right)^{1/2} \quad (7)$$

$$k_{\Phi} = \left(\frac{1}{2c^2D}\left([(c^3\mu_{\mathrm{a}} - 3\omega^2D)^2 + (c^2\omega + 3c\omega\mu_{\mathrm{a}}D)^2]^{1/2}\right.\right.$$
$$\left.\left. - (c^3\mu_{\mathrm{a}} - 3\omega^2D)\right)\right)^{1/2} \quad (8)$$

The equivalent formulations of eqns. (7) and (8) given by Fishkin et al.[10] contain a denominator of $(c\mu_{\mathrm{a}} - 3\omega^2Dc^{-2})$, which causes significant problems in data analysis if $c\mu_{\mathrm{a}} = 3\omega^2Dc^{-2}$. This is identical to $\mu_{\mathrm{a}}(\alpha\mu_{\mathrm{a}} + \mu'_{\mathrm{s}}) = \omega^2/c^2$ and correspondents to the use of high modulation frequencies in very weak absorbing and scattering media. As we have no physical relevance for this pole, we avoid it in our expressions.

If a detection fiber is placed at distance r perpendicular to $\boldsymbol{r}$ and parallel to the emission fiber (cf. Fig. 1), the detected signal is proportional to the photon density. In the following,
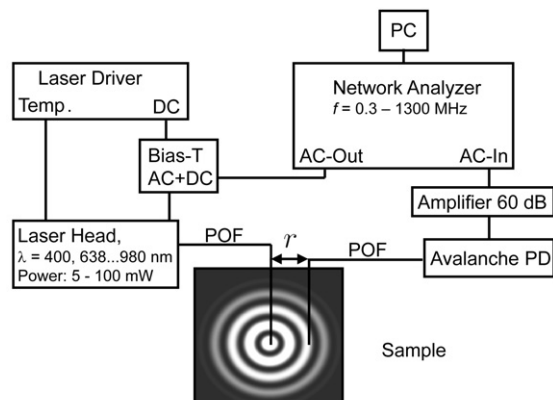

Fig. 1 Scheme of the experimental setup with a PDW sketch.

the detected amplitude of the time-depending part of this signal will be called ac-intensity and denoted with $I_{\mathrm{AC}}(r)$.

$$I_{\mathrm{AC}}(r) \propto \frac{C}{r}\exp(-k_{\mathrm{I}}r) \quad (9)$$

The proportionality constant contains experimental characteristics, such as detector efficiency, geometry parameters, etc. The phase shifting terms are summed to the phase shift $\Phi(r)$:

$$\Phi(r) = k_{\Phi}r - \Phi_0 \quad (10)$$

With a certain reference distance r_0, one obtains from eqn. (9) after linearization:

$$\ln\frac{I_{\mathrm{AC}}(r)r}{I_{\mathrm{AC}}(r_0)r_0} = -k_{\mathrm{I}}(r - r_0) \quad (11)$$

Analogous treatment of the phase shift leads to:

$$\Phi(r) - \Phi(r_0) = k_{\Phi}(r - r_0) \quad (12)$$

For data analysis the distance dependance of the ac-intensity $I_{\mathrm{AC}}(r)$ and of the phase shift $\Phi(r)$ are used to determine the intensity and phase coefficients k_{I} and k_{Φ}. From k_{I} and k_{Φ}, the absorption coefficient μ_{a} and the reduced scattering coefficient μ'_{s} can be obtained by a nonlinear fitting procedure.

3 Experimental

3.1 Apparatus

In our PDW spectrometer, intensity-modulated laser diodes with wavelengths λ between 400 and 980 nm and optical powers from 5 to 100 mW are used as inexpensive light sources with high spectral intensity. A similar experimental approach was used by Pham et al.[14] Each laser diode is mounted in a self-assembled laser head, which provides temperature stabilization, collimation and coupling into a plastic optical fiber (POF). An optical narrow bandwidth filter can be inserted to suppress spontaneous broadband emission. Temperature control and dc-current are supported by a laser diode driver (LDC8002/TED8040, Profile Optische Systeme, Karlsfeld, Germany). A network analyzer (8712 ET, Agilent, Böblingen, Germany) provides a modulation signal with frequencies from 300 kHz to 1.3 GHz and detects ac-intensity and phase shift. The minimal acquisition time at a detection bandwidth of 15 Hz is 60 ms per data point. A bias-T (ZFBT4R2GW, Mini-Circuits, Brooklyn, USA) is used to add the modulation signal to the dc-current of the laser driver just before the laser head. The POF carrying the laser light (emission fiber, 1 mm diameter) is inserted into the sample under investigation. A second POF (detection fiber, 1 mm diameter), which is arranged

perpendicular to, and at the same height as, the emission fiber, guides the scattered light to a silicon avalanche photodiode module (APM-400P, Becker&Hickl, Berlin, Germany) providing a gain factor of approximately 80. After further amplification by a 60 dB high-frequency amplifier (HSA-Y-1-60, Femto, Berlin, Germany) with a maximal bandwidth of 1.1 GHz, the electrical signal is detected by the network analyzer. In order to avoid detection of luminescence, an optical bandwidth filter can be inserted between detection fiber and avalanche photo diode. A linear translation stage (M410CG, PI, Karlsruhe, Germany) with a repeatability of 2 μm is used to set various distances between the detection and the emission fiber. Network analyzer, translation stage, switching between different laser heads and data acquisition are controlled by a computer. The experiments reported here were performed with a laser diode (HL6323MG, Hitachi, Tokyo, Japan) emitting 35 mW at 639 nm. For data analysis, the mean values of ten measurements were used, resulting in a acquisition time of approximately 0.6 s per data point. Sample volumes used for the PDW investigations ranged from 0.1 to 2 l. A scheme of the experimental setup is depicted in Fig. 1.

The extinction measurements were performed with a commercial absorption spectrometer (Cary500Scan, Varian, Darmstadt, Germany). In order to minimize effects of multiple scattering, $\mu_s l$ was always kept in the single-scattering regime by using cuvettes with different optical path lengths. All spectra were corrected by the extinction of a cuvette filled with water. For fluorescence measurements a commercial fluorescence spectrometer (Fluoromax3, Yobin Yvon, Longjumeau, France) with quantum efficiency correction was used. All measurements were performed at 293 K.

3.2 Compounds

The model media introduced here consisted of isosulfan blue (dye content approximately 90%, Sigma-Aldrich, Munich, Germany) and polystyrene beads as absorbing and scattering compound, respectively. All ISB concentrations used for this study were prepared from the same stock solution with a concentration of 5 mM. The PS-beads were synthesized by emulsion polymerization of styrene in water with sodium dodecyl sulfate as emulsifier and potassium peroxodisulfate as starter. After 6 h polymerization at 120 °C under reflux, any unpolymerized monomer was removed by a rotary evaporator. Then the samples were dialyzed for one week against water to remove ions and emulsifier. The particle size can be varied by the concentration of emulsifier and starter. A higher concentration of starter or emulsifier results in a smaller particle size. The extinction measurements were carried out with PS-beads of 0.04 μm radius, while the PS-beads used for the PDW experiments had a radius of 0.13 μm. Oxazine 170 (Radiant Dyes, Wermelskirchen, Germany) was used as a reference dye for determination of luminescence quantum yields. All the water used in this work was purified and deionized (Milli-Q Synthesis, Millipore, Schwalbach, Germany).

4 Results

4.1 Characterization of model systems

The quality of investigations of model media strongly depends on the appropriate choice and careful characterization of the compounds. In order to adjust the absorption and reduced scattering coefficients of the model samples predictably and independently from each other and other influences, the following restrictions were imposed to find a suitable absorber and scatterer: (1) negligible scattering of the absorber and absorption of the scatterer, (2) high molar absorption coefficient and specific scattering coefficient to minimize the concentrations necessary for the desired optical properties, (3) least

possible influence of scatterer or absorber concentration and temperature on the molar absorption coefficient and specific scattering coefficient, (4) negligible luminescence quantum yield of the absorber, to avoid propagation of light with different wavelengths, as this light is subject to other absorption and scattering coefficients, (5) availability of different scatterer sizes to study their effect on light propagation, and (6) low tendency of the scatterer for sedimentation or aggregation. These requirements will be discussed in detail in the following.

(1) The contribution of scattering of ISB can be roughly estimated by extinction measurements of concentrated ISB solutions in a wavelength range where absorption is small. The molar extinction spectrum of ISB is depicted in Fig. 2. For small particles exhibiting Rayleigh scattering, the specific scattering coefficient shows a λ^{-4} dependance. Even if the extinction of ISB at 850 nm would only be caused by scattering, the molar extinction coefficient of approximately 3.4 mm^{-1} M^{-1} allows to estimate the molar scattering coefficient at 639 nm to be smaller than 11 mm^{-1} M^{-1}, which is negligible *versus* absorption. In the following, the extinction of ISB will thus be assigned to absorption.

The determination of the absorption coefficient of PS-beads by extinction measurements seems rather difficult, but the high transparency of bulk polystyrene indicates a negligible specific absorption coefficient. In the context of its use in optical fibers, Zubia *et al.* report an attenuation coefficient due to absorption for polystyrene of 26 dB km^{-1} at 672 nm.[15] This corresponds to a specific absorption coefficient of 6×10^{-6} mm^{-1}. Therefore, the extinction of the PS-beads will be assigned to scattering.

(2) The molar absorption coefficient of ISB has a strong peak with $\varepsilon = (20.9 \pm 0.3) \times 10^3$ mm^{-1}M^{-1} at 639 nm, which is exactly matching the emission wavelength of one of our laser diodes. The error is estimated from repeated measurements. For a given particle size and wavelength, the specific scattering coefficient of a scatterer depends mainly on the relative refractive index of the scatterer m_{Sca} relative to the medium ($m_{Sca} = n_{Sca}/n$), which is $m \approx 1.2$ for PS-beads in water at 639 nm. Although aqueous suspensions of many inorganic compounds (*e.g.* rutile) do have a much higher relative refractive index, their application as model compounds is often restricted by sedimentation and aggregation effects.

(3) In order to investigate the dependance of the molar absorption coefficient of ISB on the concentration of ISB, molar absorption spectra were calculated from extinction spectra recorded at different ISB concentrations. For concentrations from 1 to 100 μM, no effect of the concentration on the molar absorption spectrum in the range of 400 to 800 nm is found. In the temperature range of 290 to 330 K, the molar
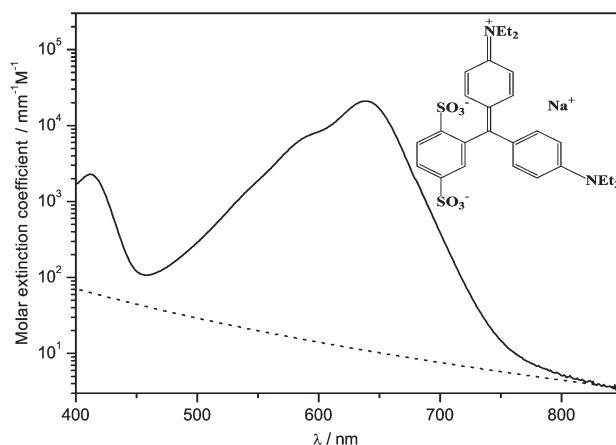
Fig. 2 Molar extinction spectrum of ISB (semi-logarithmic) with the maximal molar scattering coefficient extrapolated from 850 nm (dotted line). The inset shows the chemical structure of ISB.

absorption coefficient of ISB at 639 nm decreases linearly with approximately 45 mm^{-1} M^{-1} K^{-1}. Therefore, samples were always investigated at 293 K. At least for small scatterer concentrations, the influence of varying absorber and scatterer concentrations on the specific scattering or molar absorption coefficient can be investigated by extinction measurements. Several mixtures of PS-beads and ISB with constant relation of their concentrations were prepared. Using a constant product of ISB or PS-bead concentration and optical path length, the same extinction is found over the whole spectral range (Fig. 3). These results indicate, that the optical properties of PS-beads and ISB are not affected by interactions in the investigated concentration range. Here, PS-beads with a rather small radius (0.04 μm) were used, as small particles have a lower specific scattering coefficient and therefore allow investigations up to a higher volume fraction in the single-scattering regime.

(4) A good indication for a low fluorescence quantum yield of ISB is the triphenyl methane structure, as dyes with this moiety often have low luminescence quantum yields. Investigations of the luminescence quantum yield of ISB were performed in reference to an ethanolic solution of oxazine 170 in different dilutions under appropriate experimental conditions. From the quantum yield of oxazine 170 in ethanol of 0.60,[16] it can be estimated that the luminescence quantum yield of ISB is well below 5×10^{-4}.
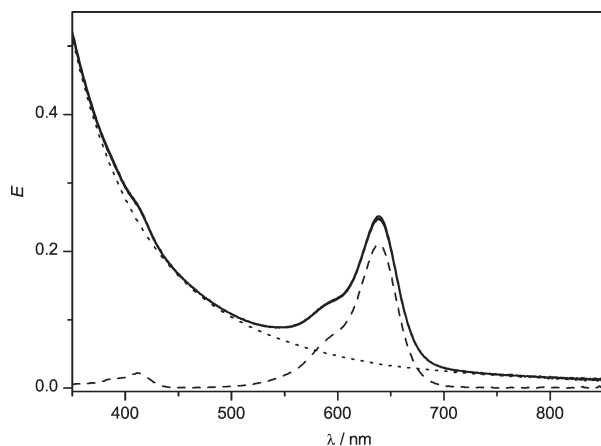
(5) The particle size of the PS-beads was characterized by a combination of dynamic light scattering and turbidimetry techniques. Both techniques indicate a monomodal particle size distribution for the PS-beads used in this work with radii of 0.04 and 0.13 μm, respectively. An more detailed characterization will be given elsewhere.

(6) The stability of the PS-beads against sedimentation or aggregation can be estimated by extinction measurements at different times after sample preparation. Although no change could be detected for days, the model media were usually investigated immediately after mixing and were kept in motion with a magnetic stirrer.

In conclusion, mixtures of ISB and PS-beads in water are very well suited as absorbing and scattering model media.

4.2 Investigations with photon density waves

4.2.1 ac-intensity and phase shift measurements. The dependencies of the ac-intensity and the phase shift on the distance r between emission and detection fiber were investigated for several model samples. For these experiments, PS-beads with a radius of 0.13 μm were used, as the reduced scattering coefficient of large PS-beads is less affected by particle–particle interactions. For a given frequency, the linear distance dependencies predicted by eqns. (11) and (12) are confirmed over the whole frequency range employed (Fig. 4).

For a given distance, higher modulation frequencies lead to decreasing ac-intensity and increasing phase shift. From the slopes of the linear fits, the intensity and phase coefficients, k_I and k_Φ, can be obtained.

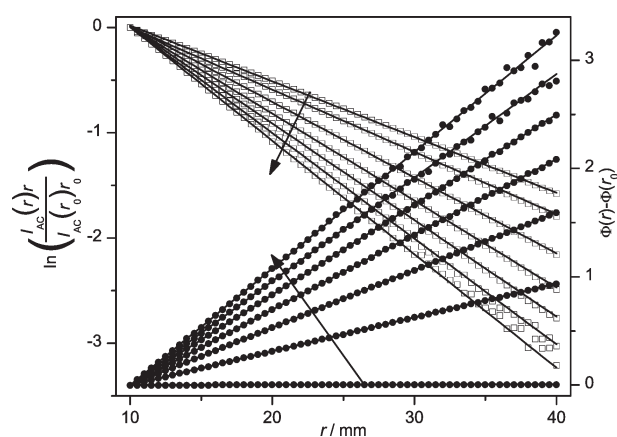**4.2.2 Variation of absorber and scatterer concentrations.** For samples with different ISB concentrations, intensity and phase coefficients as well as nonlinear fits according to eqns. (7) and (8) are shown in Fig. 5.

The intensity coefficients increase with rising absorption, as the photon density waves are more and more damped by the stronger absorption. In parallel, the phase coefficients decrease, as photons travelling a long path and therefore carrying a large phase delay are more likely to be absorbed than others taking a more direct way. The absorption and reduced scattering coefficients, μ_a and μ_s', obtained from the intensity and phase coefficients by non-linear fitting are shown in Fig. 6.

For samples with different PS-bead volume fractions, intensity and phase coefficients and nonlinear fits according to eqns. (7) and (8) are shown in Fig. 7.

The phase coefficients increase with stronger scattering, as enhanced scattering enlarges the mean path of the detected photons and therefore their phase delay. The intensity coefficients also raise with increasing reduced scattering coefficients, because the longer path length travelled by the photons leads to a stronger damping by absorption. The absorption and reduced scattering coefficients obtained from the intensity and phase coefficients by non-linear fitting are shown in Fig. 8.

The results presented in Figs. 6 and 8 support the following observations and conclusions: (1) For a constant PS-bead concentration, μ_s' remains constant, for example, at *ca.* 0.73 mm^{-1} with a standard deviation of about 0.8% in Fig. 6. (2) For variable scatterer concentrations, μ_s' is exactly proportional to the PS-bead volume fraction (Fig. 8). Thus, the measurement of μ_s' allows the accurate determination of the scatterer concentration. (3) Considering absorption properties, it is obvious from Fig. 8 that for constant ISB concentrations, μ_a reduces from 0.011 to 0.009 mm^{-1} up to a PS-bead volume fraction of

Fig. 3 Extinction spectra of mixtures with PS-bead volume fractions of 7.5×10^{-6}, 1.5×10^{-5}, 3.75×10^{-5} and 7.5×10^{-5} and 1, 2, 5 and 10 μM ISB using 10, 5, 2 and 1 mm optical path length, respectively. The four spectra are indistinguishable from each other. The extinction spectra of an aqueous solution of ISB (dashed) and PS-beads (dotted) are given for comparison.

Fig. 4 Evaluation of ac-intensity (open squares, left axis) and phase shift (filled circles, right axis) according to eqns. (11) and (12) at 70 distances plotted in reference to $r_0 = 10$ mm for modulation frequencies increasing along the arrows from 0.3 to 1248 MHz with linear fits (lines). The sample contained 0.188 μM ISB and a PS-bead volume fraction of 5.5×10^{-4}.
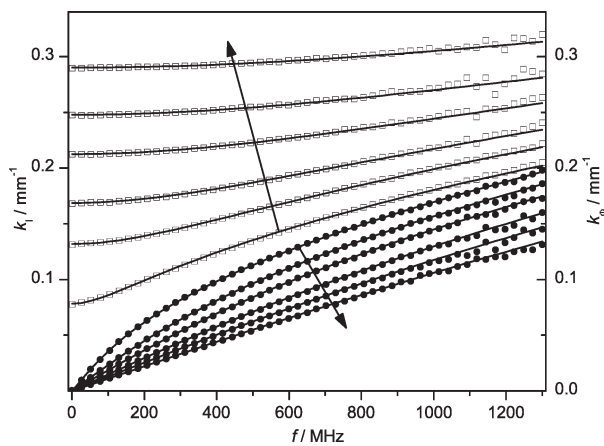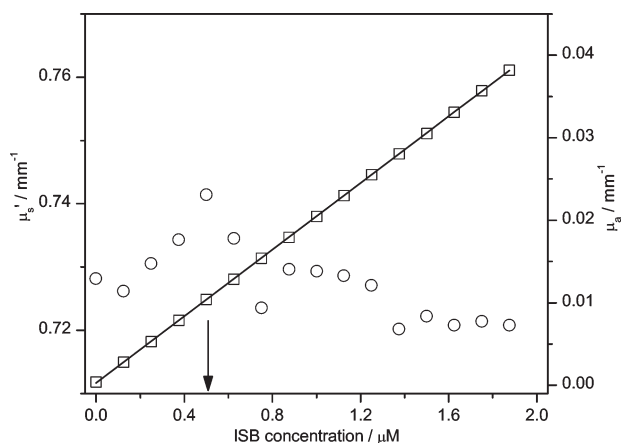
Fig. 5 Intensity (open squares, left axis) and phase coefficients (filled circles, right axis) of samples differing in their ISB concentrations with nonlinear fits (lines). The arrows indicate the increase of [ISB] from 0.13 to 1.88 μM, while the PS-bead volume fraction was kept at 1.8×10^{-3}.

Fig. 7 Intensity (open squares, left axis) and phase coefficients (filled circles, right axis) of samples differing in their PS-bead concentration with nonlinear fits (lines). The arrows indicate the increase of the PS-bead volume fraction from 7.3×10^{-4} to 3.6×10^{-2}, while the ISB concentration was 0.5 μM.
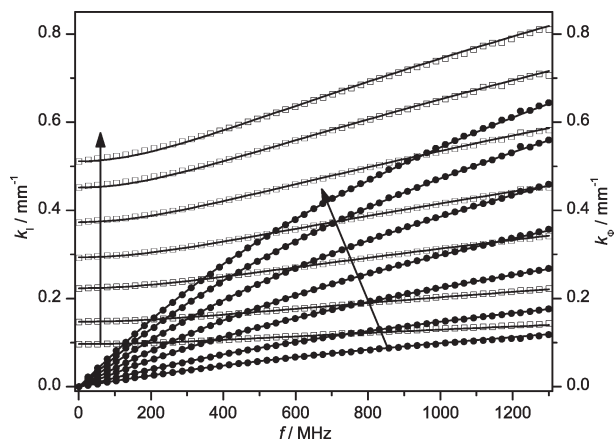
0.036, which amounts to an effect of *ca.* 20%. (4) On the other hand, μ_a exhibits excellent linearity with ISB concentrations from 0.13 to 1.88 μM (Fig. 6). However, the molar absorption coefficient obtained from the slope, $\varepsilon_{ISB} = (20.19 \pm 0.02) \times 10^3$ mm^{-1}M^{-1}, appears to be significantly below the value from the dye absorption spectrum $\varepsilon_{ISB} = (20.9 \pm 0.3) \times 10^3$ mm^{-1}M^{-1}. This slight dependance of ε_{ISB} on the PS-bead concentration translates into a *ca.* 3% deviation at a PS-bead volume fraction of 0.0018. (5) Under representative absorption and scattering conditions, for example $\mu_a = 0.02$ mm^{-1} and $\mu_s' = 0.7$ mm^{-1}, the experimental precision of μ_a and μ_s' is estimated to be better than 1%.

5 Conclusions

The conducted investigations show that our multi-frequency domain PDW spectrometer and data analysis using the P1 approximation to the Boltzmann transport equation enable independent determination of the absorption and reduced scattering coefficients. Mixtures of ISB and PS-beads in water are well suited as absorbing and scattering model media. This is especially supported by the low luminescence quantum yield of ISB and the absence of optically detectable interactions
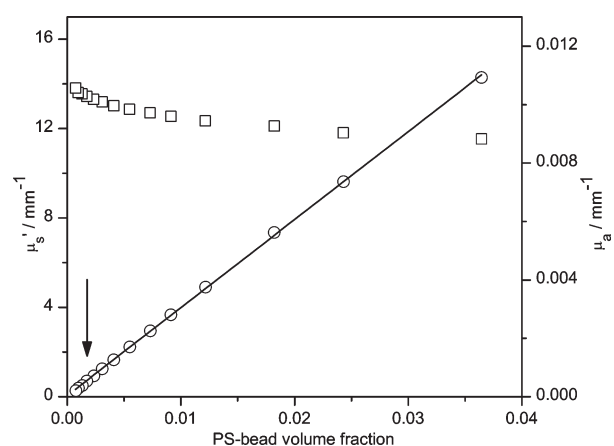
of the components at low scatterer concentrations. Under multiply scattering conditions, the excellent precision allows the observation of a dependance of ε_{ISB} on the PS-bead concentration. This may be caused by errors in the determination of μ_a due to approximations in the theoretical treatment or due to experimental conditions, or by an influence of PS-beads on ISB properties. While it is presently difficult to discriminate between these sources, we feel that changes of the ISB molar absorption coefficient are most important, as the PS-beads probably slightly modify macroscopic solvent parameters influencing ISB photophysical properties. The absence of the effect at low PS-bead concentrations, *e.g.* in the extinction measurements, indicates, that it is rather related to the volume fraction of the PS-beads than to their surface. The negative charge on both, the dye and the PS-beads, should also prevent an adsorption to the surface. Since the absorption coefficient is a linear function of the ISB concentration, a determination of the ISB concentration is still possible if the dependance of ε_{ISB} on the PS-bead volume fraction is accounted for. Over the range of PS-bead concentrations investigated, the reduced scattering coefficient is a linear function of the PS-bead volume fraction. At higher concentrations, a deviation due to particle-particle interaction is expected.

Fig. 6 Reduced scattering coefficient μ_s' (circles, left axis) and absorption coefficient μ_a (squares, right axis) obtained for samples only differing in their ISB concentration. The line is a linear fit to the absorption coefficient with an intercept of $(3.0 \pm 0.2) \times 10^{-4}$ mm^{-1} and a slope of $(20.19 \pm 0.02) \times 10^3$ mm^{-1}M^{-1}. The arrow indicates the ISB concentration used in the measurements plotted in Figs. 7 and 8.

Fig. 8 Reduced scattering coefficient (circles, left axis) and absorption coefficient (squares, right axis) obtained for samples only differing in their PS-bead concentration. The line is a linear fit to the reduced scattering coefficient with an intercept of (0.05 ± 0.02) mm^{-1} and a slope of (394 ± 1) mm^{-1}. The arrow indicates the PS-bead volume fraction which was used for the experiments displayed in Figs. 5 and 6.

Acknowledgements

References

1 E. Wagner, R. Dändliker and K. Spenner, in *Sensors*, ed. W. Göpel, J. Hesse and J. N. Zemel, VCH, Weinheim, 1992, vol. 6.
2 J. B. Fishkin and E. Gratton, *J. Opt. Soc. Am. A*, 1993, **10**, 127–140.
3 B. J. Tromberg, L. O. Svaasand, T. Tsay and R. C. Haskell, *Appl. Opt.*, 1993, **32**, 607–616.
4 M. A. O'Leary, D. A. Boas, B. Chance and A. G. Yodh, *Phys. Rev. Lett.*, 1992, **69**, 2658–2661.
5 J. M. Schmitt, A. Knüttel and J. R. Knutson, *J. Opt. Soc. Am. A*, 1992, **9**, 1832–1843.
6 L. O. Svaasand, B. J. Tromberg, R. C. Haskell, T. Tsay and M. W. Berns, *Opt. Eng.*, 1993, **32**, 258–266.
7 M. S. Patterson, J. D. Moulton, B. C. Wilson, K. W. Berndt and J. R. Lakowicz, *Appl. Opt.*, 1991, **30**, 4474–4476.
8 Z. Sun, S. Torrance, F. K. McNeil-Watson and E. M. Sevick-Muraca, *Anal. Chem.*, 2003, **75**, 1720–1725.
9 Y. Huang and E. M. Sevick-Muraca, *J. Colloid Interface Sci.*, 2002, **251**, 434–442.
10 J. B. Fishkin, S. Fantini, M. J. vandeVen and E. Gratton, *Phys. Rev. E*, 1996, **53**, 2307–2319.
11 G. Mie, *Ann. Phys.*, 1908, **25**, 377–445.
12 O. Reich and F. Schael, *Proc. SPIE-Int. Soc. Opt. Eng.*, 2001, **4431**, 299–305.
13 D. J. Durian, *Opt. Lett.*, 1998, **23**, 1502–1504.
14 T. H. Pham, O. Coquoz, J. B. Fishkin, E. Anderson and B. J. Tromberg, *Rev. Sci. Instrum.*, 2000, **71**, 2500–2513.
15 J. Zubia and J. Arrue, *Opt. Fib. Technol.*, 2001, **7**, 101–140.
16 R. Sens and K. H. Drexhage, *J. Lumin.*, 1982, **24/25**, 709–712.